# Spectrum Channel Characterization Using Delay and Doppler Spread Parameters

Hector Reyes[1], Naima Kaabouch[1], and Wen-Chen Hu[2]
[1]Department of Electrical Engineering, University of North Dakota, Grand Forks 58203, USA
[2]Department of Computer Science, University of North Dakota, Grand Forks 58203, USA
Email: hector.reyesmoncayo@my.und.edu; naima.kaabouch@engr.und.edu; wenchen@computer.org

***Abstract*—**This paper describes a non-blind technique, channel sounder, to characterize a wireless channel. This technique is based on the transmission of a pseudo random sequence through the channel, the calculation of its autocorrelation to estimate the channel impulse response, and from it the calculation of the Delay and Doppler spread parameters. This channel sounder was implemented using GNU radio software and software defined radio units (USRP N200). Experiments were performed at different scenarios: an anechoic chamber, a parking lot, and a street. The results show that in absence of interference or multipath the Delay and Doppler Spread parameters were zero; however they differed from zero with interference, attenuation, and multipath. These results show that the technique could be used to characterize and qualify available spectrum channels, since the measurements can reflect not only multipath but also other factors such as interference and attenuation.

***Index Terms*—**Delay spread, doppler spread, channel characterization, autocorrelation.

## I. Introduction

The characterization of radio channels becomes instrumental for the configuration and operation of wireless networks. Knowing the channel characteristics allows for the planning and adjustment of operation parameters of radio equipment, including transmission techniques, bandwidth, transmission power, bit rates and others. Since a wireless channel behaves as a filter, its impulse response, known as channel impulse response (CIR), can characterize it. In order for a radio to adjust its parameters to the environment, it needs to update the impulse response of the channel of interest as often as possible. Methods for estimating the CIR can be classified in two types: blind and non-blind methods.

The blind methods obtain the channel response estimate without sending any pilot or training sequence. These methods estimate this response out of the received samples. Maximum likelihood (ML) can perform well in blind estimation [1], [2]; however they are computationally expensive. A few methods have been proposed to reduce the processing time, including Cyclic ML [2], Boolean Quadratic Program [3], and Expectation-Maximization [4], [5]. Other techniques such as subspaces [6], second order statistics [7], and high order statistics [8] have also contributed to the improvement of blind estimation.

On the other hand, non-blind estimation uses a pilot or training sequence to estimate the CIR. This approach is one of the most intensively studied methods for time-varying channels [9]. A pilot is a previously known signal located in the time domain for single carrier systems and in the frequency domain for multicarrier systems. Some of the most prevalent pilot aided estimators are: linear minimum square error (LMMSE) estimator [10], [11], the least square (LS) estimator, and the best linear unbiased estimator (BLUE) [12]. All these methods use a previously known sequence and the received signal to estimate the response of the channel. Another method is the correlation sounding technique, which takes advantage of the statistical properties of pseudo noise sequences and employs autocorrelation to estimate the channel impulse response [13].

In the literature previously referenced, the authors exposed their methods supporting them with simulations and sometimes experiments; they assumed that their results came only from the configuration and movement of obstacles and scatterers. This paper focuses not only on explaining Delay Spread and Doppler Spread calculations but also on showing how interference can impact the results. The remainder of this paper is organized as follows: Section 2 explains the methodology followed to perform the channel characterization; Section 3 summarizes and discusses the results; and Section 4 gives the conclusion.

## II. Methodology

### A. Channel Impulse Response

The channel is characterized by estimating the channel impulse response (CIR) and calculating two parameters from it: Doppler Spread and Delay Spread, which condense the information provided by the CIR. These parameters lead us to the *coherence bandwidth* and *coherence time*. The coherence bandwidth, $B_c$, imposes restrictions over the bandwidth of the signal to transmit through the channel. Likewise, the coherence time, $T_c$

Manuscript received November 25, 2013; revised March 12, 2014.
This work was supported by the North Dakota Experimental Program to Stimulate Competitive Research, ND EPSCoR, National Science Foundation, NSF, under grant EPS-0184442, and Rockwell Collins under grant UND0017909
Corresponding author email: hector.reyesmoncayo@my.und.edu
doi:10.12720/jcm.9.3.234-240

limits the symbol time [14]. Matz and Hlawatsch [12] provide a definition of the coherence bandwidth and the coherence time as shown in equation (1).

$$B_c = \frac{1}{S_\tau}, \qquad T_c = \frac{1}{S_\nu} \tag{1}$$

where $S_\tau$ and $S_\nu$ represents the Delay Spread and Doppler Spread respectively.

Knowing $B_c$, $S_\tau$, $T_c$, and $S_\nu$ helps the communication system -for instance, a cognitive radio- to adapt its operating configuration to fit better with the current conditions of the channel.

The channel impulse response (CIR) – represented as $h(t,\tau)$ in equation 2 – indicates the number of paths used by the signal to propagate, the attenuation on each path, and the relative delay between paths.

$$h(t,\tau) = \sum_{i=1}^{L} a_i(t)\delta(\tau - \tau_i) \tag{2}$$

where $t$ is the time, $\tau$ is the delay, $a_i(t)$ is the time varying complex attenuation for the path $i$, the delta function $\delta(\tau - \tau_i)$ represents the path $i$ with delay $\tau_i$, and $L$ is the number of paths [15]. The Fourier transform of $h(t,\tau)$ with respect to $t$ yields $s(\nu,\tau)$ – the scattering function – which shows the change of the paths and the shift of the central frequency due to the Doppler effect.

### B. Condense Parameters of the Channel

The Delay spread and the Doppler spread are the normalized second order central moments of the power delay profile (PDP) and the Doppler power spectrum (DPS) [14], [16], [17]. To calculate PDP and DPS $h(t,\tau)$ and $s(\nu,\tau)$ are considered stochastic processes, which is necessary, since they are unpredictable in the practice [12]. To simplify $h(t,\tau)$ and $s(\nu,\tau)$ we use the autocorrelation function (ACF) and assume that the channel is wide sense stationary – uncorrelated scattering (WSSUS) [12], [18]. For instance, by applying the ACF to $h(t,\tau)$ we have [16]

$$R_h(t_1,t_2,\tau_1,\tau_2) = E[h(t_1,\tau_1)h^*(t_2,\tau_2)] \tag{3}$$

where $h^*$ is the complex conjugate of $h$ and $E[\cdot]$ is the expected value operation. The WSSUS model, which is broadly accepted for mobile channels [18], has two assumptions. The first assumption is that the stochastic process is wide sense stationary, WSS, which implies that the ACF depends only on $\Delta t = t_2 - t_1$, and not on the absolute time, $t$. Therefore, equation (3) becomes

$$R_h(\Delta t,\tau_1,\tau_2) = E[h(t,\tau_1)h^*(t+\Delta t,\tau_2)] \tag{4}$$

The second assumption is that the amplitudes and phases of the different paths are uncorrelated, which means the channel has uncorrelated scattering, US. Therefore, the ACF is zero when $\tau_1 \neq \tau_2$ and has a peak when $\tau_1 = \tau_2$. By applying this assumption to equation (4) it becomes

$$R_h(\Delta t,\tau) = E[h(t,\tau)h^*(t+\Delta t,\tau)] \tag{5}$$

which calculated at $\Delta t = 0$ yields the function $p_h(\tau) = R_h(\tau) = R_h(\tau,0)$ or *power delay profile* –PDP [16]. The PDP represents the distribution of the power among the delayed paths of the signal arriving at the receiver. By normalizing the PDP, it turns into a probability density function, designated as $p(\tau)$. Equation (6) shows this normalization.

$$p(\tau) = \frac{R_h(\tau)}{\int_{-\infty}^{\infty} R_h(\tau)d\tau} = \frac{p_h(\tau)}{\int_{-\infty}^{\infty} p_h(\tau)d\tau} \tag{6}$$

The normalized second order central moment of $p(\tau)$ is:

$$S_\tau = \sqrt{\int_{-\infty}^{\infty} (\tau - D_\tau)^2 p(\tau)d\tau} \tag{7}$$

the *delay spread*. In equation (7)

$$D_\tau = E[\tau] = \int_{-\infty}^{\infty} \tau p(\tau)d\tau \tag{8}$$

is the *mean delay*. Since in the practice, only a limited number of discrete signals avail, we use the discrete versions of equations (7) and (8) as given by [16], [19]

$$S_\tau = \sqrt{\frac{\sum (\tau_i - D_\tau)^2 p_h(\tau_i)}{\sum p_h(\tau_i)}} \tag{9}$$

where

$$D_\tau = \frac{\sum \tau_i p_h(\tau_i)}{\sum p_h(\tau_i)} \tag{10}$$

A similar process works when calculating the Delay Spread $-S_\nu$; the integral of the scattering function $s(\nu,\tau)$ with respect to $\tau$ yields $p_D(\nu)$, known as the Doppler spectrum. The equations (6) to (10) applied to $p_D(\nu)$ return $S_\nu$.

### C. Estimation of the Channel Impulse Response and the Condense Parameters of the Channel

To estimate $h(t,\tau)$, $S_\tau$, and $S_\nu$ a pseudo-random (PN) sequence is transmitted through the channel and its autocorrelation calculated at the receiver. This method bases on the fact that the autocorrelation of white noise is an impulse [20]. Since sending white noise through a channel is impractical, we used a signal PN sequence because its autocorrelation resembles the autocorrelation of white noise [13]. Fig. 1 shows that the transmitter and receiver combine of GNU Radio software along with a USRP (Universal Software Radio Peripheral) unit. The USRP TX sends a PN sequence through a channel with response $h(t,\tau)$. The USRP RX takes the signal from the channel, processes and delivers it to the PN correlator block that calculates the autocorrelation to obtain $\hat{h}(t,\tau)$

– an estimate of $h(t,\tau)$. The next block takes this estimate to calculate $S_\tau$ and $S_\nu$ using the aforementioned equations.

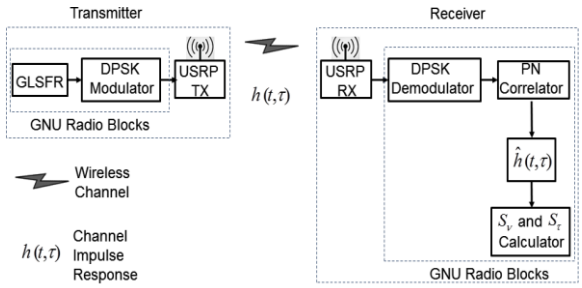


Fig. 1. Block diagram of the channel sounder.

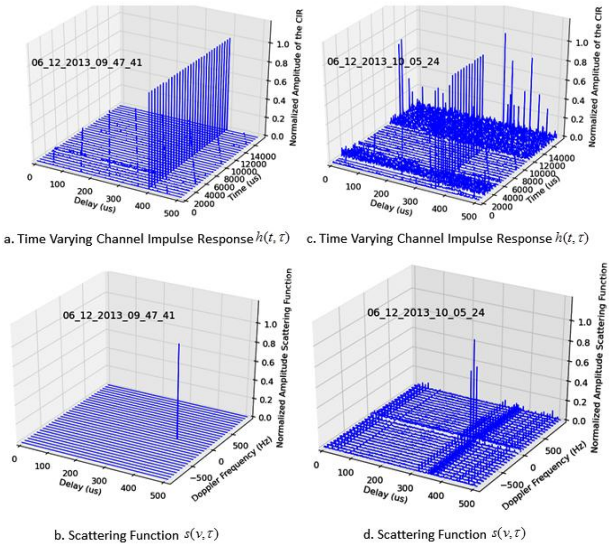


Fig. 2. Example of channel impulse response and scattering function obtained in a parking lot. (a) and (b) show only one path and no Doppler shift; (c) and (d) show multiple paths and Doppler shift.

The PN sequence originates from a Galois linear feedback shift register (GLFSR) generator [21]. A GLFSR generator has a polynomial, whose degree $n$ determines the length sequence $L$ according to $L = 2^n - 1$. The GLFSR and PN correlator blocks have both two parameters: mask and degree, which must agree to calculate a autocorrelation, otherwise the PN correlator would calculate the cross-correlation. The configuration used for the experiments was: degree 9 and mask 0 to get a 511 bits long autocorrelation sequence. Each autocorrelation sequence represents the channel impulse response at certain instant $t_i$. Several of these sequences arranged one after another form $h(t,\tau)$. Fig. 2 in the next section illustrates examples of $h(t,\tau)$ and $s(\nu,\tau)$.

## III. Results and Discussion

The experiments were performed at different environments – an anechoic chamber, a parking lot surrounded by buildings, and a street located between two parking lots – and at the frequencies: 850MHz, 1910MHz, 2410MHz and 5850MHz. The two first frequencies are commonly used in cellphone networks and two last ones belong to the group of ISM (Industrial, Scientific, and Medical) bands, which are unlicensed and prevalently used in wireless networks, such as Wi-Fi, Bluetooth and Zigbee. The Delay and Doppler spread were calculated every 8 seconds, 220 times per each experiment. The experiments in the anechoic chamber were performed with and without interference; a signal generator was adjusted at 5 and 10 dBm to create two levels of interference. The outdoor experiments were made in the morning and in the afternoon observing the surrounding activity, such as movement of cars and people (their portable devices), in order to see how the results were affected.

Fig. 2 provides examples of the channel impulse response $h(t,\tau)$ and scattering function $s(\nu,\tau)$ obtained during the experiments performed in the parking lot. As one can see Fig. 2a and Fig. 2b show only one path and no Doppler shift, whereas Fig. 2c and Fig. 2d show multiple paths and Doppler shifts. The sampling rate was configured to one million of samples per second, which set the bit rate at 1 Mbps and the time resolution at 1 µs. Fig. 2a and Fig. 2c show how $h(t,\tau)$ forms from putting each autocorrelation one after another along the axis, *"Time (us)"*. Since each autocorrelation sequence is 511 bits long and the time of bit is 1 µsec, its duration is 511 µsec. Therefore, $h(t,\tau)$ is sampled every 511 µsec, which corresponds to the sampling time, $T_{samp}$. The inverse of $T_{samp}$ is the sampling rate, $F_s$, which is 1956 Hz. Fig. 2b and Fig. 2d illustrate $s(\nu,\tau)$, the Fourier transform of $h(t,\tau)$ with respect to time. Since $F_s$ is 1956 Hz, the axis *"Doppler frequency* (Hz)*"* in figures 2b and 2d ranges between $-F_s/2$=978 Hz and $F_s/2$=978 [22].

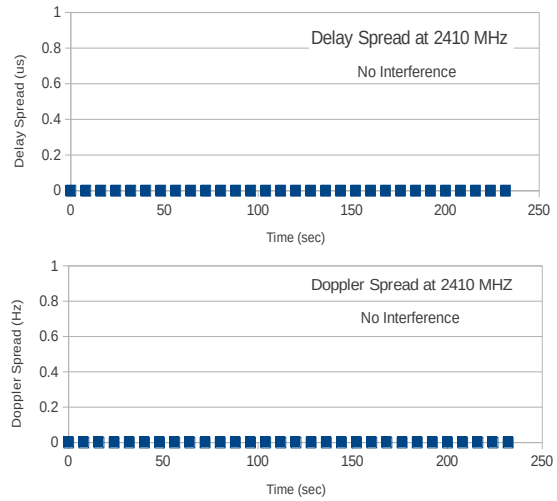


Fig. 3. Example of results at the anechoic chamber with no signal generator.

### A. Experiments in Controlled Environment

Fig. 3 shows the Delay and Doppler Spread functions in the anechoic chamber. As expected in such environment free of reflections and movement, the Delay and Doppler spreads were zero. Fig. 4 and Fig. 5 show examples of results obtained using a continuous signal as a source of interference. As expected, the Delay and Doppler functions consistently differed from zero and

concentrated around the average value. Experiments performed at other frequencies - 5850 MHz, 1910 MHz, and 850 MHz - yielded similar results, Delay and Doppler spread functions were equal to zero in absence of interference, whereas with interference they always differed from zero and their averages increased as the power of the interference increased.

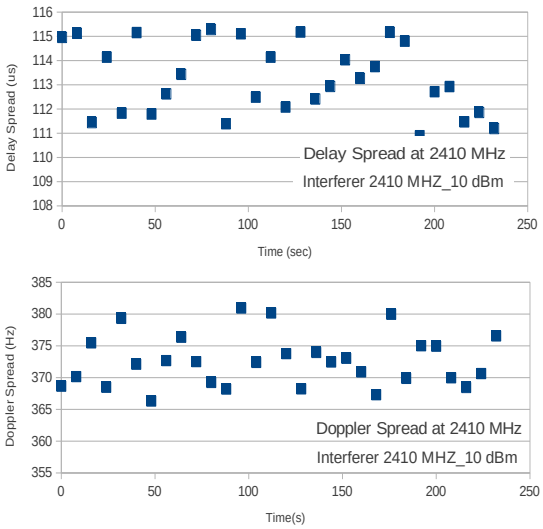


Fig. 4. Example of results at the anechoic chamber with signal generator at 10 dBm.

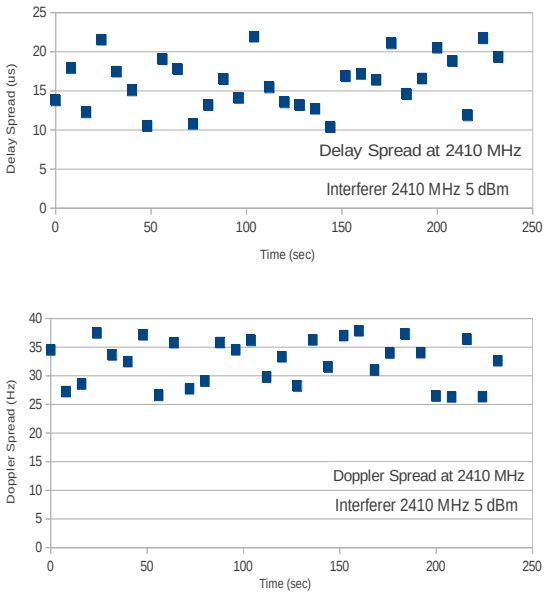


Fig. 5. Example of results at the anechoic chamber with signal generator at 5 dBm.

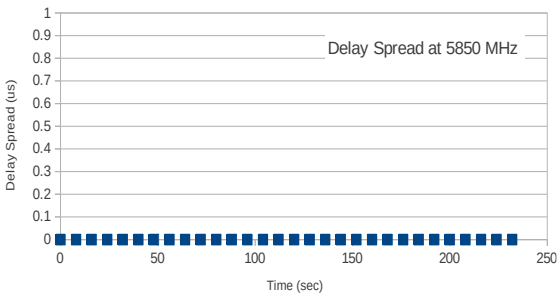


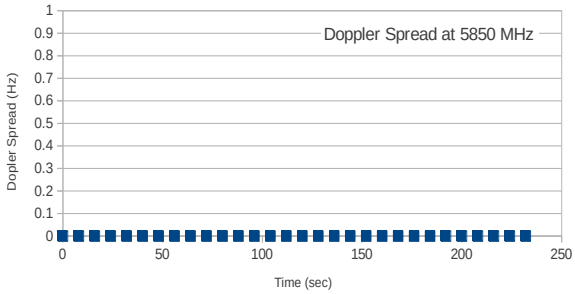


Fig. 6. Example of results obtained in the parking lot surrounded by buildings at 5850 MHz.

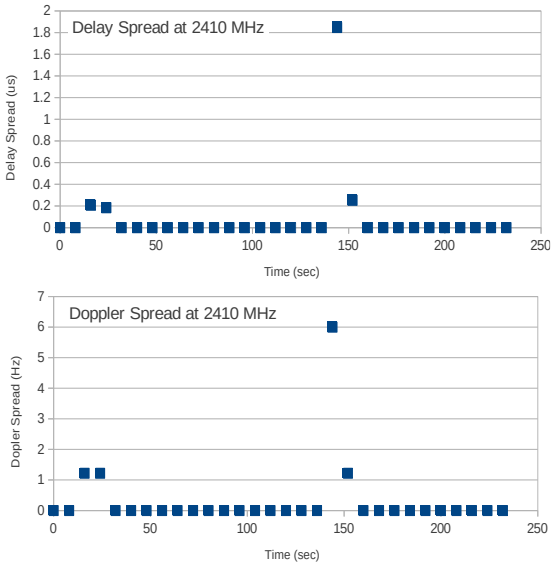


Fig. 7. Example of results obtained in the parking lot surrounded by buildings at 2410MHz.

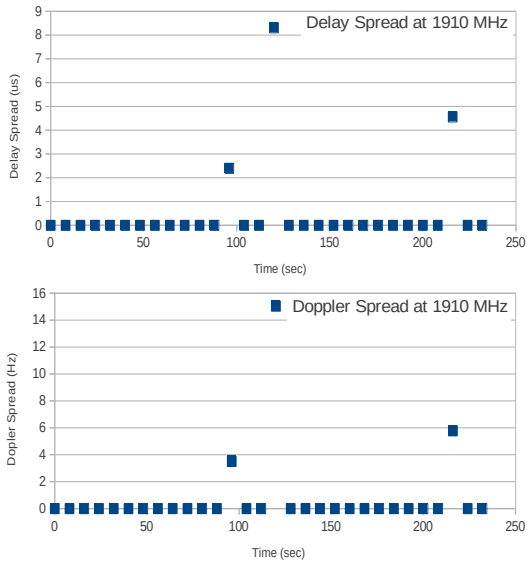


Fig. 8. Example of results obtained in the parking lot surrounded by buildings at 1910 MHz.

## B. Experiments in Outdoor Environment

Fig. 6 through Fig. 9 give examples of results obtained in a parking lot at 5850 MHz, 2410 MHz, 1910 MHz and 850 MHz during the afternoon. Experiments performed during the morning produced similar behavior. As one

can see, most of the results were zero and the few non-null values ranged in a wide scope. Fig. 10 through Fig. 13 give examples of the results obtained in a street located between two parking lots at the same frequencies comport alike.

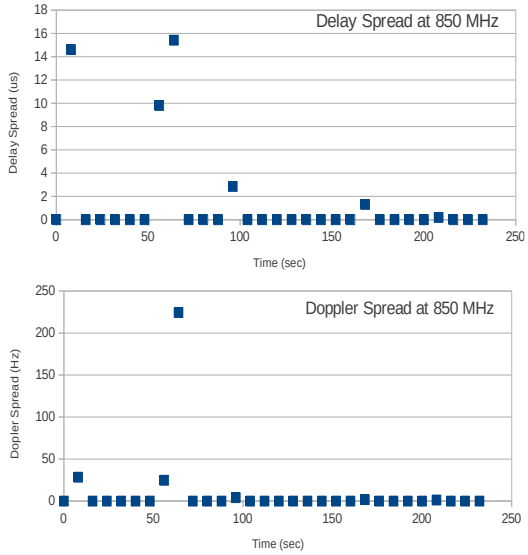


Fig. 9. Example of results obtained in the parking lot surrounded by buildings at 850 MHz.

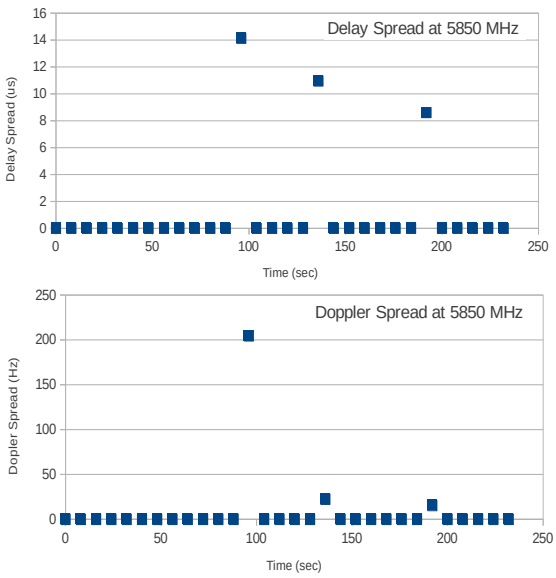


Fig. 10. Example of results for experiments obtained in a street between two parking lots at 5850 MHz.

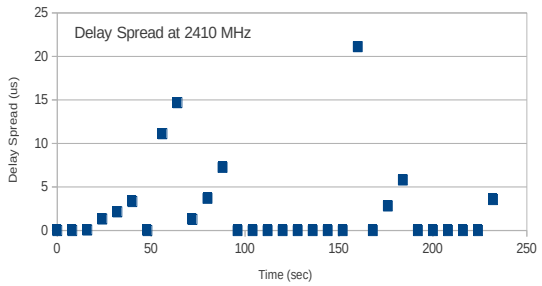


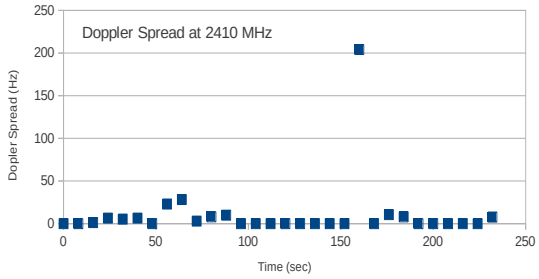


Fig. 11. Example of results for experiments obtained in a street between two parking lots at 2410 MHz.

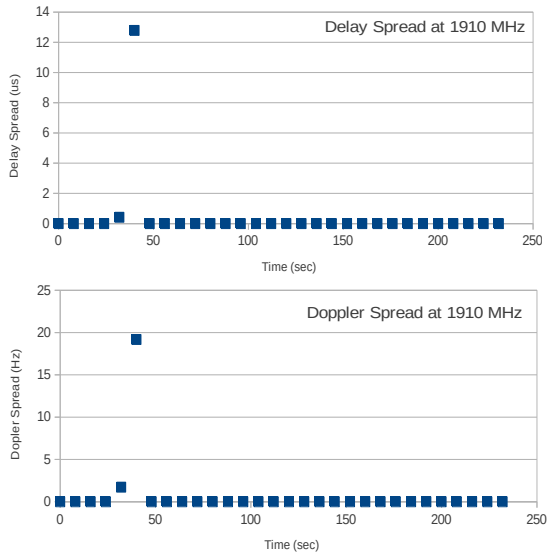


Fig. 12. Example of results for experiments obtained in a street between two parking lots at 1910 MHz.

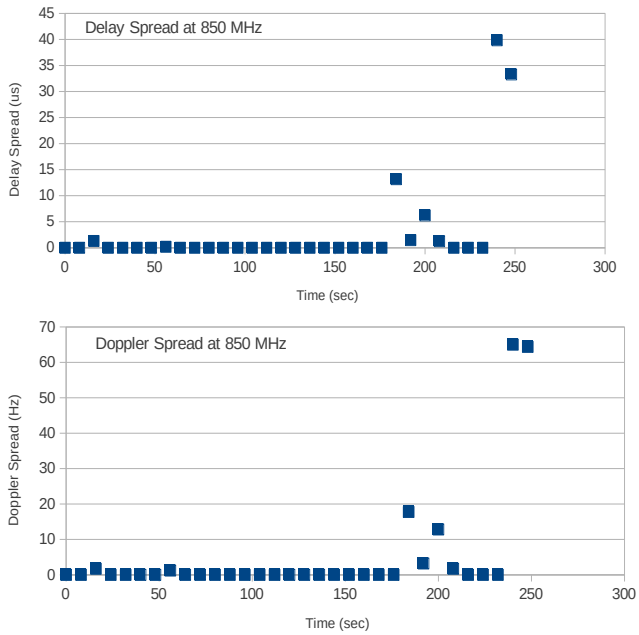


Fig. 13. Example of results for experiments obtained in a street between two parking lots at 850 MHz.

TABLE I: AVERAGE DELAY SPREAD, DOPPLER SPREAD AND PERCENTAGE OF NON-NULL RESULTS

| Frequency (MHz.) | Scenario and Conditions* | AVG_Del** (µsec.) | AVG_Dopp** (Hz.) | Non-null ** (%) |
|---|---|---|---|---|
| 5810 | Parking Lot_Morning | 0.00 | 0.07 | 0.9 |
| | Parking Lot_Afternoon | 0.00 | 0.00 | 0 |
| | Street_Morning | 0.42 | 1.98 | 4.5 |
| | Street_Afternoon | 0.52 | 2.15 | 5.4 |
| 2410 | Anechoic Chamber- No interference | 0.00 | 0.00 | 0.00 |
| | Anechoic Chamber_5 dBm | 16.27 | 31.58 | 100 |
| | Anechoic Chamber_10 dBm | 113.14 | 373.27 | 100 |
| | Parking Lot_Morning | 0.39 | 0.30 | 5 |
| | Parking Lot_Afternoon | 0.08 | 0.29 | 7.2 |
| | Street_Morning | 1.00 | 3.45 | 8.2 |
| | Street_Afternoon | 0.96 | 3.59 | 9 |
| 1910 | Parking Lot_Morning | 0.04 | 0.08 | 0.9 |
| | Parking Lot_Afternoon | 0.15 | 0.25 | 3.2 |
| | Street_Morning | 0.23 | 0.40 | 4.1 |
| | Street_Afternoon | 0.13 | 0.23 | 2.3 |
| 850 | Parking Lot_Morning | 0.29 | 0.89 | 4 |
| | Parking Lot_Afternoon | 0.43 | 1.94 | 5.4 |
| | Street_Morning | 1.43 | 2.50 | 7.2 |
| | Street_Afternoon | 0.89 | 1.57 | 6.4 |

***Conditions** can be the presence and absense of interference; or morning and afternoon

****AV_Del:** Average of Delay Spread ; **AV_Dopp**: Average of Delay Spread; **Non-Null:** Percentage of non-null numbers

** Averages and percentages calculated out of 220 numbers

Table I shows that in the anechoic chamber the results for Delay and Doppler spread rose around eight times when the power of the signal generator increased by 5 dB. In the other scenarios – outdoors without controlled interference – the numbers were much lower and equaled zero in most of the cases. In most cases, the numbers obtained in the street exceeded the numbers obtained in the parking lot. 2410 MHz registered the highest values, whereas 5850 MHz registered the lowest. For the outdoor scenarios the values changed from morning to afternoon, although in some cases the change was small, such as at 5850 MHz in the parking lot and at 2410 MHz in the street. Table I shows that in the anechoic chamber the results for Delay and Doppler spread rose around eight times when the power of the signal generator increased by 5 dB. In the other scenarios – outdoors without controlled interference – the numbers were much lower and equaled zero in most of the cases. In most cases, the numbers obtained in the street exceeded the numbers obtained in the parking lot. 2410 MHz registered the highest values, whereas 5850 MHz registered the lowest. For the outdoor scenarios the values changed from morning to afternoon, although in some cases the change was small, such as at 5850 MHz in the parking lot and at 2410 MHz in the street.

### C. Discussion

In presence of interference, the results obtained at the anechoic chamber for Delay and Doppler spread differed consistently from zero. This means that interference influenced the results given by the channel sounder, since the anechoic chamber is an environment free of reflections and scatterers. The impact of the interference on the results depends on its intensity as shown in table 1. In the outdoor experiments the outcomes also agreed with what we expected; the results mostly equated zero, which makes sense, considering that the distances between the channel sounder and sources of multipath or Doppler shift, such as reflectors and scatterers, were less than 300 meters, distance needed to have delays of 1 µsec – the time resolution of our channel sounder. However, some results differed from zero. For instance, some Doppler Spread results differed from zero even in absence of movement, which means they must have come from interference.

During the outdoor experiments we observed an association between the frequency and the non-null results. For example, the percentages of non-null results at 2410 MHz exceeded those obtained at 5850 MHz. This observation coincides with the fact that 2410 MHz is more common than 5850 MHz. At 1910 MHz the results were smaller compared to those at 850 MHz. A possible explanation is that the higher the frequency, the higher the propagation losses; therefore, at 1910 MHz the signal and the interference are more attenuated, which can explain the results shown in table 1 and figures 6 to 13. The non-null results obtained in the outdoor experiments were fewer and sparser than those obtained in the anechoic chamber, because in the anechoic chamber the interference was constant, whereas in the outdoor scenarios it was intermittent and changed its intensity randomly. Another association observed during these experiments was between the transit of cars and non-null Delay and Doppler spread results; in the experiments performed in the street, when the cars passed between transmitter and receiver the results differed from zero. A possible explanation for this is that the cars attenuated the signal and/or created multipath signals as they interrupted the line of sight between the transmitter and receiver affecting the results.

## IV. CONCLUSIONS

This paper describes a non-blind technique to characterize a wireless channel. This technique is based on the transmission of a pseudo random sequence through the channel, the calculation of its autocorrelation at the receiver to estimate the channel impulse response, and the calculation of the Delay and Doppler spread. Experiments showed that interference and attenuation of the sounding signal caused by obstacles affected the results. The results show that the proposed method can be exploited to acquire better knowledge of the channel and the environment where a communication system is working at.

Future work includes experiments in other environments with larger distances that can generate delays bigger than 1 µsec; it also includes setups where we can move the transmitter and receiver of the channel sounder controlling and registering their relative speed and angles. We also should consider the sampling rate in future experiments, since this parameter can help in assessing if the outcomes indicate real delays and Doppler shifts or if they have been affected by other factors. It is also important to determine which and how other factors affect the characterization of the channel so that we can exploit the results to have better knowledge about the channel and its environment.

## ACKNOWLEGMENTS

We acknowledge the support of North Dakota-Experimental Program to Stimulate Competitive Research, ND EPSCoR, National Science Foundation, NSF, under grant EPS-0184442, and Rockwell Collins under grant UND0017909.


## REFERENCE


[1] E. G. Larsson, P. Stoica, and J. Li, "On maximum-likelihood detection and decoding for space-time coding systems," *IEEE Trans. on Signal Processing*, vol. 50, no. 4, pp. 937-944, 2002.

[2] E. G. Larsson, P. Stoica, and J. Li, "Orthogonal space-time block codes: Maximum likelihood detection for unknown channels and unstructured interferences," *IEEE Trans. on Signal Processing*, vol. 51, no. 2, pp. 362-372, 2003.

[3] W. Ma, B. Vo, T. N. Davidson, and P. Ching, "Blind ML detection of orthogonal space-time block codes: Efficient high-performance implementations," *IEEE Trans. on Signal Processing*, vol. 54, no. 2, pp. 738-751, 2006.

[4] A. Gallo, E. Chiavaccini, F. Muratori, and G. M. Vitetta, "BEM-based SISO detection of orthogonal space-time block codes over frequency flat-fading channels," *IEEE Trans. on Wireless Communications*, vol. 3, no.6, pp. 1885-1889, 2004.

[5] Y. Li, C. N. Georghiades, and G. Huang, "Iterative maximum-likelihood sequence estimation for space-time coded systems," *IEEE Trans. on Communications*, vol. 49, no.6, pp. 948-951, 2001.

[6] N. Ammar and Z. Ding, "Blind channel identifiability for generic linear space-time block codes," *IEEE Trans. on Signal Processing*, vol. 55, no. 1, pp. 202-217, 2007.

[7] J. Vía, I. Santamaría, and J. Pérez, "Code combination for blind channel estimation in general MIMO-STBC systems," *EURASIP Journal on Advances in Signal Processing*, pp. 3, 2009.

[8] V. Choqueuse, A. Mansour, G. Burel, L. Collin, and K. Yao, "Blind channel estimation for STBC systems using higher-order statistics," *IEEE Trans. on Wireless Communications*, vol. 10, no. 2, pp. 495-505, 2011.

[9] G. Leus, Z. Tang, and P. Banelli, "Estimation of time-varying Channels–A block approach," in *Wireless Communications Over Rapidly Time-Varying Channels*, F. Hlawatsch and G. Matz, Academic Press, pp. 155-194, 2011.

[10] N. Geng, X. Yuan, and L. Ping, "Dual-diagonal LMMSE channel estimation for OFDM systems," *IEEE Trans. on Signal Processing*, vol. 60, no. 9, pp. 4734-4746, 2012.

[11] K. Hung and D. W. Lin, "Pilot-based LMMSE channel estimation for OFDM systems with Power–Delay profile approximation," *IEEE Trans. on Vehicular Technology*, vol. 59, no. 1, pp. 150-159, 2010.

[12] G. Matz and F. Hlawatsch, "Fundamentals of time-varying communication channels," in *Wireless Communications Over Rapidly Time-Varying Channels*, F. Hlawatsch and G. Matz, Academic Press, pp. 1-63, 2011.

[13] R. J. Pirkl and G. D. Durgin, "Optimal sliding correlator channel sounder design," *IEEE Trans. on Wireless Communications*, vol. 7, no. 9, pp. 3488-3497, 2008.

[14] A. F. Molisch. *Wireless Communications*, 2nd Edition, John Wiley & Sons, 2010.

[15] A. F. Molisch, L. J. Greenstein, and M. Shafi, "Propagation issues for cognitive radio," in *Proc. IEEE*, vol. 97, no. 5, pp. 787-804, 2009.

[16] F. P. Fontán and P. M. Espieira, *Modelling the Wireless Propagation Channel: A Simulation Approach with MATLAB*, Wiley, 2008.

[17] R. Narasimhan and D. C. Cox, "A generalized doppler power spectrum for wireless environments," *IEEE Communications Letters*, vol. 3, no. 6, pp. 164-165, 1999.

[18] S. Saunders and A. Aragón-Zavala, *Antennas and Propagation for Wireless Communication Systems*, John Wiley & Sons, 2007.

[19] T. S. Rappaport, *Wireless Communications: Principles and Practice*, Prentice Hall, 2002.

[20] H. Stark and J. W. Woods, *Probability and Random Processes with Application to Signal Processing*, Prentice Hall, 2002.

[21] M. Goresky and A. M. Klapper, "Fibonacci and Galois representations of feedback-with-carry shift registers," *IEEE Trans. on Information Theory*, vol. 48, no. 11, pp. 2826-2836, 2002.

[22] S. Salous, *Radio Propagation Measurement and Channel Modelling*, John Wiley & Sons, 2013


**Hector Reyes** was born in Bogotá, Colombia**.** He received his Electronics Engineering and Master in Telematics degrees from the Universidad Distrital Francisco Jose de Caldas in 1998 and 2003 respectively. He is currently pursuing his Ph.D. degree at the Department of Electrical Engineering of the University of North Dakota. His research interests include Cognitive Radio, Wireless sensors Networks and Rural Telecommunications.

**Naima Kaabouch** is currently an associate professor in the Electrical Engineering Department at the University of North Dakota, Grand Forks, USA. She received her B.S. and M.S. degrees in electrical engineering from the University of Paris 11 as well as and a Ph.D. in electrical engineering from the University of Paris 6, France. Her research interests include signal/image processing, sensing, smart systems, wireless communications and cognitive radio.

**Wen-Chen Hu** is currently an associate professor in the Department of Computer Science of the University of North Dakota, Grand Forks. He received a PhD in Computer Science from the University of Florida, Gainesville, in 1998. His current research interests include handheld-mobile/smartphone/tablet computing, location-based services, Web-enabled information systems such as search engines and Web mining, electronic and mobile commerce systems, and Web technologies.